Heliyon 10 (2024) e28022

Contents lists available at ScienceDirect

Heliyon

journal homepage: www.cell.com/heliyon

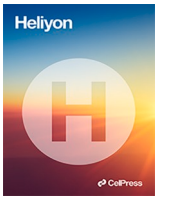

Research article

Integration of network pharmacology and experimental verifications reveals the Bian-Se-Tong mixture can alleviate constipation in STC rats by reducing apoptosis of Cajal cells via activating PI3K-Akt signaling pathway

Rong Wu [a,1], Zhibin Zhang [b,1], Qingxia Xu [a], Fang Liu [a,b], Yu Zhan [a], Qiuxiao Wang [b], Lijuan Du [c,d,**], Xuegui Tang [b,*]

[a] Hospital of Chengdu University of Traditional Chinese Medicine, Chengdu 611130, China
[b] North Sichuan Medical College, Nanchong 637000, China
[c] Department of Anorectal, Affiliated Hospital of Southwest Jiaotong University, Chengdu 610000, China
[d] Department of Anorectal, Chengdu Thrid People's Hospital, Chengdu 610000, China

ARTICLE INFO

Keywords:
Network pharmacology
Slow-transit constipation
Molecular mechanism
PI3K/AKT pathway
Apoptosis

ABSTRACT

Bian-Se-Tong mixture (BSTM) is an optimized formulation based on the classical prescription "Zhizhu pill", which is widely used in the clinical treatment of slow-transit constipation (STC). The potential molecular mechanism of BSTM therapy for STC was investigated by network pharmacology prediction combined with animal experiments. The active components of BSTM were screened via the TCMSP platform. The GeneCards, OMIM and DrugBank databases were used to search for STC targets. With the help of the Biogenet tool, a protein interaction network between drugs and disease targets was constructed, and the intersection network of the two was extracted to obtain the key targets of BSTM in the treatment of STC. GO and KEGG enrichment analyses of key targets were carried out with Metascape. Loperamide hydrochloride was used to establish an STC rat model, and the key targets and related pathways were preliminarily verified. The important signaling pathways included the PI3K-Akt, MAPK, IL-17, cAMP, and cell cycle signaling pathways. The experimental results showed that BSTM treatment increased the body weight of STC rats and increased the fecal particle number, fecal water content and intestinal carbon ink promotion rate within 24 h. Further pathological changes in the colon of the rats were also observed. In-depth mechanistic studies have shown that BSTM can significantly reduce the apoptosis of intestinal Cajal cells, downregulate the expression of Bax and c-Caspase 3, upregulate the expression of Bcl-2 and c-kit, and promote the phosphorylation of AKT. The results showed that BSTM can significantly relieve constipation in STC rats via a mechanism related to activating the PI3K-Akt signaling pathway and improving Cajal cell apoptosis.

* Corresponding author. North Sichuan Medical College, Nanchong, P.R. 637000, China.
** Corresponding author. The Third People's Hospital of Chengdu, Chengdu 611130, China.
E-mail addresses: dulijuan4937@163.com (L. Du), txg668nc@sohu.com (X. Tang).
[1] These authors contributed equally to this paper.

https://doi.org/10.1016/j.heliyon.2024.e28022
Received 10 November 2023; Received in revised form 9 March 2024; Accepted 11 March 2024
Available online 13 March 2024

1. Introduction

Slow-transit constipation (STC) is a functional disease characterized by reduced peristalsis of the colon and reduced intestinal transport capacity, resulting in retention of stool in the intestine [1–3]. In traditional Chinese medicine, dry stool, hard stool, difficult defecation and other diseases are regarded as STC, and its treatment has always followed the principles of preserving Wei Qi, preserving Jin Ye and rational drug use. The pathogenesis of STC is complex, and modern studies suggest that STC is related mainly to the intestinal nervous system, Cajal interstitial cells of the colon, some hormones, gastrointestinal neurotransmitters, intestinal flora, intestinal smooth muscle and other mental and psychological factors, which influence each other to form a complex network [3–7]. At present, the clinical treatment of STC is not exact, and the long-term effect of this treatment is poor. Natural medicine shows great potential in the treatment of human diseases. Traditional Chinese medicine (TCM) is a traditional natural medicine from China that has multiple components and multiple targets and has obvious advantages in the treatment of STC [8].

Bian-Se-Tong mixture (BSTM) is a mixture of prescribed drugs created based on the classic prescription "Zhizhu pill", which includes Atractylodes macrocephala Koidz, Nelumbo nucifera Gaertn., Magnolia officinalis Rehd. et Wils., Rehmannia., and Citrus aurantium L., and it is widely used in the clinical treatment of STC. BSTM contains many flavonoids, alkaloids, polyphenols, lignin and other components. Moreover, current pharmacological studies have shown that BSTM can regulate aquaporins, substance P, vasoactive peptides and other indicators in STC rats, thus affecting colonic motility and water metabolism [9–11]. However, the specific mechanism of BSTM in the treatment of STC is still unclear. Network pharmacology combines systems biology and computer technology to systematically and comprehensively analyze the mechanism and material basis of natural drugs to improve disease efficacy [12]. This study used network pharmacology to predict and analyze the main active ingredients and potential action targets of BSTM to improve STC incidence and verified its targets and signaling pathways through in vivo experiments to provide a basis for further revealing its pharmacodynamic ingredients and pharmacological effects.

2. Materials and methods

2.1. Materials

All Chinese medicines were obtained from the Pharmacy of Chinese Medicine of the Affiliated Hospital of North Sichuan Medical College and were certified by the Pharmacy to meet the standards of the Chinese Medicine Pharmacopoeia. All the herbs were identified by Prof. Xuegui Tang. The specimens were kept in the herbarium of the Affiliated Hospital of North Sichuan Medical College. Bifidobacterium Sanxian Live bacteria capsules were obtained from Shanghai Xinyi Pharmaceutical Co., Ltd. Loperamide hydrochloride capsules (LOPs) were obtained from Xi 'an Janssen Pharmaceutical Co., Ltd.

2.2. Screening of the active components of BSTM

The TCM system pharmacology database TCMSP is a powerful platform for TCM component analysis [13]. In the TCMSP database, the chemical constituents and their target points of Atractylodes macrocephala Koidz. (BZ), Nelumbo nucifera Gaertn. (HY), Magnolia officinalis Rehd. et Wils. (HP), Rehmannia. (SDH), and Citrus aurantium L. (ZS) were searched. Moreover, the CNKI database was used to search for these drugs via keywords, and recent related literature reports were consulted to determine the underlying factors and targets of the drugs. The criteria for screening active ingredients were set an oral bioavailability (OB) $\geq$30% and drug likeness (DL) $\geq$0.18 [14]. After all the effective components of traditional Chinese medicine and their targets were collected, the component library and target library of BSTM were preliminarily obtained by removing duplicate values.

2.3. STC target retrieval and collection

The terms "slow transit constipation" or "STC" were entered into the GeneCards, OMIM, and DrugBank human disease gene databases for retrieval. The disease gene results were collected, and duplicate values were removed. Thus, a disease target library was obtained.

2.4. Visualization of drug component-target interactions

The component-target data pair of BSTM was imported into Cytoscape 3.8.1 software [15], and the Network Analyzer function of the software was used to construct an interaction diagram between the active components of BSTM and the target.

2.5. Construction of the protein interaction network

The BSTM target library and STC target library were imported into Cytoscape 3.8.1 software, the protein interaction network diagram of the target was constructed by using the function of the BisonGenet plug-in, and the connectivity centrality (DC), mediocrity centrality (BC) and compactness centrality (CC) were calculated to further screen the key targets. Using the BisonGenet plug-in function of Cytoscape 3.8.1 software, an STC protein interaction network diagram and a drug component target protein interaction network diagram were constructed. After the interaction network diagram of the two proteins was constructed, the Mergr plug-in function was used to visualize the overlap of the two network diagrams. According to the DC, BC and CC results in the database,

the overlapping targets were screened successively to obtain the key targets.

2.6. Analysis of biological processes and enrichment pathways

Gene Ontology (GO) analysis and Kyoto Encyclopedia of Genes and Genomes (KEGG) pathway enrichment analysis were subsequently conducted for the selected key targets using the Metascape platform.

2.7. Animal experiment

A total of 48 male SPF-grade SD rats weighing 210–230 g were obtained from the Laboratory Animal Center of North Sichuan Medical College. The laboratory animal use license number of North Sichuan Medical College is SYXY (Sichuan) 2018-076. The animals were kept in cages in an animal central laboratory, well ventilated, lit for 12 h a day, with a relative humidity of 50 ± 50%, a temperature of 25 °C, and free access to food and water This animal experiment was approved by the Ethics Committee of North Sichuan Medical College (NSMC Ethical Animal Review 2021-10-4). Atractylodes macrocephala Koidz., Nelumbo nucifera Gaertn., Magnolia officinalis Rehd. et Wils., Rehmannia., and Citrus aurantium L. were added to a porcelain pot. Then, 800 ml of distilled water was added, and the mixture was allowed to soak for 30 min. Briefly, the mixture was boiled and simmered for 30 min. The liquid was then filtered, and 500 ml of distilled water was added again. The liquid was then brought to a simmer for 30 min. After filtering, the liquid was mixed twice and concentrated into a 1.14 g/mL decoction. The samples were sealed in a refrigerator at 4 °C for later use. After one week of adaptive feeding, 6 rats were randomly assigned to the NC group (normal control group). The remaining rats were intragastrically administered LOP, and a rat constipation model was established for 14 consecutive days. The LOP suspension was formulated with saline at a dose of 15 ml/kg twice daily. The NC group was intragastrically administered an equal volume of normal saline twice a day for 14 days. After successful modeling, the rats were randomly divided into five groups, namely, the model group (STC), Bifidobacterium group (positive), L-BSTM group (low dose), M-BSTM group (medium dose) and H-BSTM group (high dose). Drug intervention began on the 15th day. In the Bifidobacterium group (62.5 mg/kg), a low dose of each mixture (6.25 mg/kg), a medium dose of each mixture (12.5 mg/kg) and a high dose of each mixture (25 mg/kg) were administered via gavage once a day for 14 consecutive days.

2.8. Fecal particle count and fecal water content

At the end of the last treatment, the rats were raised alone in a metabolic cage, where their feces were collected every hour for 24 h, and the amount and weight of their feces were recorded. After the feces were dried in a 60 °C dryer for 12 h, the fecal moisture content was calculated according to the following formula.

$$\text{Fecal moisture content } (\%) = (\text{wet weight} - \text{dry weight})/\text{wet weight} \times 100\%.$$

2.9. Intestinal propulsion rate

The rats in each group (n = 8) were injected with charcoal powder (20 ml/kg, 3% activated carbon mixed with 0.5% methylcellulose aqueous solution) 30 min after the last gavage to evaluate intestinal motility. The rats were killed 40 min later. The calculation formula for calculating the intestinal transmission rate is as follows:

$$\text{Intestinal propulsion rate } (\%) = \text{Activated carbon intestinal travel (cm)}/\text{intestinal length (cm)} \times 100\%$$

2.10. Histopathological analysis

At the end of the experiment, the rats were killed, and part of the colon tissue was collected and fixed with 4% paraformaldehyde. Then, the tissues were paraffin embedded, and 5 μm sections were cut. After dewaxing and rehydration, hematoxylin-eosin (HE) staining was used to observe the histological morphology. The thickness of the colon mucus was measured by Periodate Schiff (PAS) staining.

2.11. TUNEL staining and immunofluorescence (IF) staining

Paraffinized colon tissue samples were sliced, and TUNEL staining was performed according to Li et al. [16]. After staining, the slices were blocked with BCA at room temperature for 2 h, incubated with drops of the c-Kit primary antibody (1 100), incubated overnight at 4 °C in a wet box, washed with PBS 3 times, incubated with the corresponding secondary antibody at room temperature for 1 h in the dark, incubated with DAPI dye solution, stained in the dark for 10 min, and incubated with antifluorescence quenching sealing tablets. The sections were observed and collected under a fluorescence microscope.

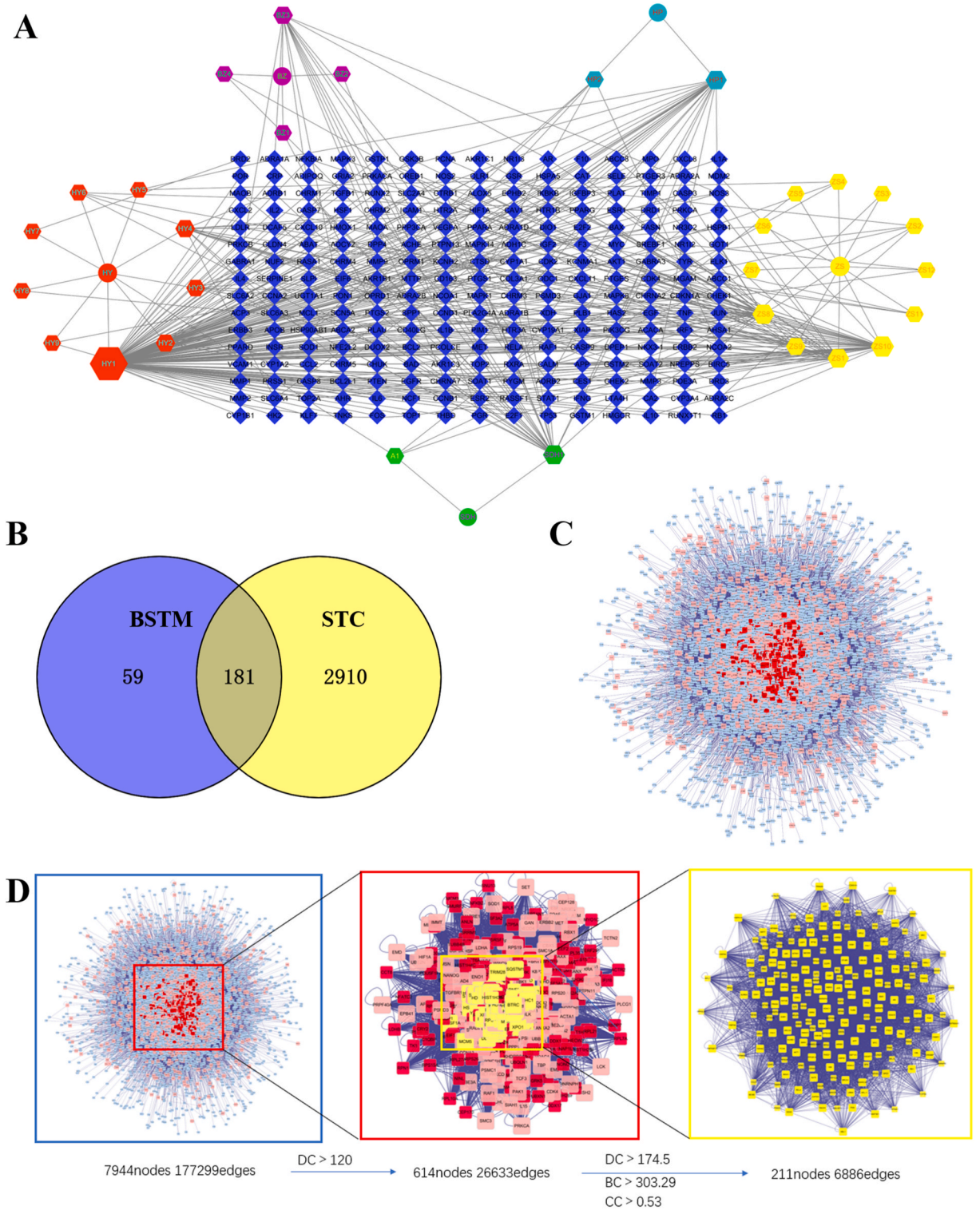

Fig. 1. Establish BSTM target, component library and STC target library. A, Interaction diagram between BSTM main active ingredients and action targets; B, Wayne diagram of drug targets and disease targets; C, Drug - Disease PPI network diagram; D, Screening process of key targets for BSTM treatment of STC.

2.12. Western blot (WB) detection

At the end of the experiment, the colon tissues of the rats were collected and immediately frozen in a −80 °C freezer. The frozen colon tissues were removed, and an appropriate amount of protein lysate was added and ground in a low-temperature abrasive solution. After grinding and centrifuging, the supernatant was collected, and the protein content of the supernatant was detected with a BCA assay kit. After preparing the WB sample, a WB experiment was carried out according to the methods of Peng et al. to detect the expression of BAX, BCL2, c-Caspase 3, PI3K, Akt, p-PI3K, *p*-Akt, c-kit, etc., in colon tissue [17].

2.13. HPLC–MS analysis

The composition of the samples was analyzed via UPLC-QE-Orbitrap-MS (Thermo, USA). Chromatographic analysis was performed on a Thermo Fisher Scientific Accucore C18 column (100 mm × 2.1 mm, 2.6 μm). The column temperature was set to 30 °C, the flow rate of the mobile phase was 1.0 mL/min, and the sample injection volume was 10 μL. The mobile phase was 0.01% acetonitrile (A)-formic acid aqueous solution (B), which was separated by the following gradient elution procedure: 0–15 min, 18% A) 15–16 min, 18–20% A) 16–20 min, 20% A) 20–21 min, 20–25% A) 21–35 min, 25% A) 35–36 min, 25–38% A) 36–45 min, 38% A) 45–46 min, 38–60% A) 46–60 min, 60% A) 60–61 min, 60-18% A) 61–80 min, 18% A. For mass spectrometry detection, the ionization source used was ESI, the scanning range was 100–1500 *m/z*, the positive ion mode spray voltage was 3500 V, the capillary temperature was 320 °C, the carrier gas was pure nitrogen, and the flow rate was 1.0 L/h.

2.14. Statistical methods

SPSS 26.0 statistical software was used for analysis, and the data are expressed as the mean ± SD. One-way analysis of variance was used to analyze the data, and the differences between groups were analyzed by a two-tailed *t*-test. $P < 0.05$ indicated a statistically significant difference.

3. Results

3.1. Acquisition of the active ingredients and targets of BSTM

A total of 428 components of BSTM were obtained, including 55 from BZ, 93 from HY, 139 from HP, 76 from SDH and 65 from ZS. After the OB and DL parameters were selected, 48 active ingredients were obtained, including 7 from BZ, 15 from HY, 2 from HP, 2 from SDH and 22 from ZS (Table S1). The predicted targets of these components were collected, and after merging, duplicate values were excluded, for a total of 240 targets.

3.2. Construction of an interaction diagram between the main active ingredients of BSTM and its active targets

The interaction diagram was constructed using Cytoscape 3.8.1 software. The purple figure represents BZ, the blue figure represents HP, the yellow figure represents ZS, the green figure represents SDH, and the red figure represents HY. A1 represents the common components of HY and SDH, and the blue figure in the middle represents the target information (Fig. 1A).

3.3. Retrieval of STC-related targets

The “slow transit constipation” or “STC” term was entered in the search field of the GeneCards, OMIM, and DrugBank human disease gene databases for retrieval; the targets were collected, the duplicate values were eliminated, and 3091 targets were ultimately selected. The intersection of 240 drug targets and 3091 disease targets was constructed into a Venn diagram, which revealed 181 DEGs (Fig. 1B).

3.4. Drug–disease PPI network diagram

With the BisonGenet plug-in function of Cytoscape 3.8.1 software, a disease protein interaction network diagram and a drug component target protein interaction network diagram were constructed. After the two protein interaction network diagrams were constructed, the overlap of the two network diagrams was obtained by using the Merge plug-in function. There were 7977 closely related targets involved in the interaction of the active components of BSTM and 178272 interaction links. There were 14571 targets closely related to the incidence of STC, and there were 251906 active relationships. The overlap of the drug-disease interaction network is shown in Fig. 1C.

3.5. The key targets for BSTM treatment of STC

Next, key targets for BSTM-mediated treatment of STC were screened. First, the median DC value was 60, a target with more than 2 times the median of 120 was retained, and 614 pieces of target information and 26633 relationships were obtained. The median DC, BC and CC values were subsequently calculated, and the target points that met the requirements of more than 174.5, 303.29 and 0.53 were

retained at the same time. Finally, 211 targets and 6886 networks were obtained. Fig. 1D shows the screening procedure, and Fig. 2A shows the final target information. Fig. 2B shows a visualization of the molecular interactions in the drug-disease PPI network.

3.6. Analysis of the biological processes and enrichment pathways associated with STC treatment by BSTM

The 211 obtained key targets were imported into the Metascape data analysis platform for analysis of GO biological processes, including cellular component and molecular function analysis. The 10 groups with the smallest *P* values were selected for plotting (Fig. 2C). Moreover, enrichment analysis of the KEGG pathways was performed, and the genes in the top 20 sites were screened by the -log10 (p value) and gene ratio. As shown in Fig. 2D, the predicted targets of the active ingredients in BSTM for improving STC efficacy were mainly involved in the PI3K-AKT signaling pathway, MAPK signaling pathway, and IL-17 signaling pathway. The color of the bubble represents the enrichment significance and the enrichment degree of the target gene in this pathway, which is expressed as the -log10 (P value). The horizontal coordinate the gene count represents the number of potential target genes belonging to the pathway.

3.7. BSTM can significantly improve the symptoms of constipation in STC rats

Analysis of the changes in body weight of the rats showed that at the end of the experiment, the body weight of the rats in the STC group was significantly lower than that of the rats in the NC group, and treatment with the positive control drug or different doses of BSTM significantly alleviated the weight loss caused by STC (Fig. 3A). The number of fecal particles, fecal water content and small intestinal charcoal thrust rate at 24 h were used to evaluate the improvement in constipation in STC rats induced by BSTM. Compared with those in the NC group, the number of fecal particles, fecal water content and small intestinal charcoal thrust rate of the rats at 24 h were significantly lower in the model group and significantly changed after intervention with various doses of BSTM ($P < 0.05$; Fig. 3B–D).

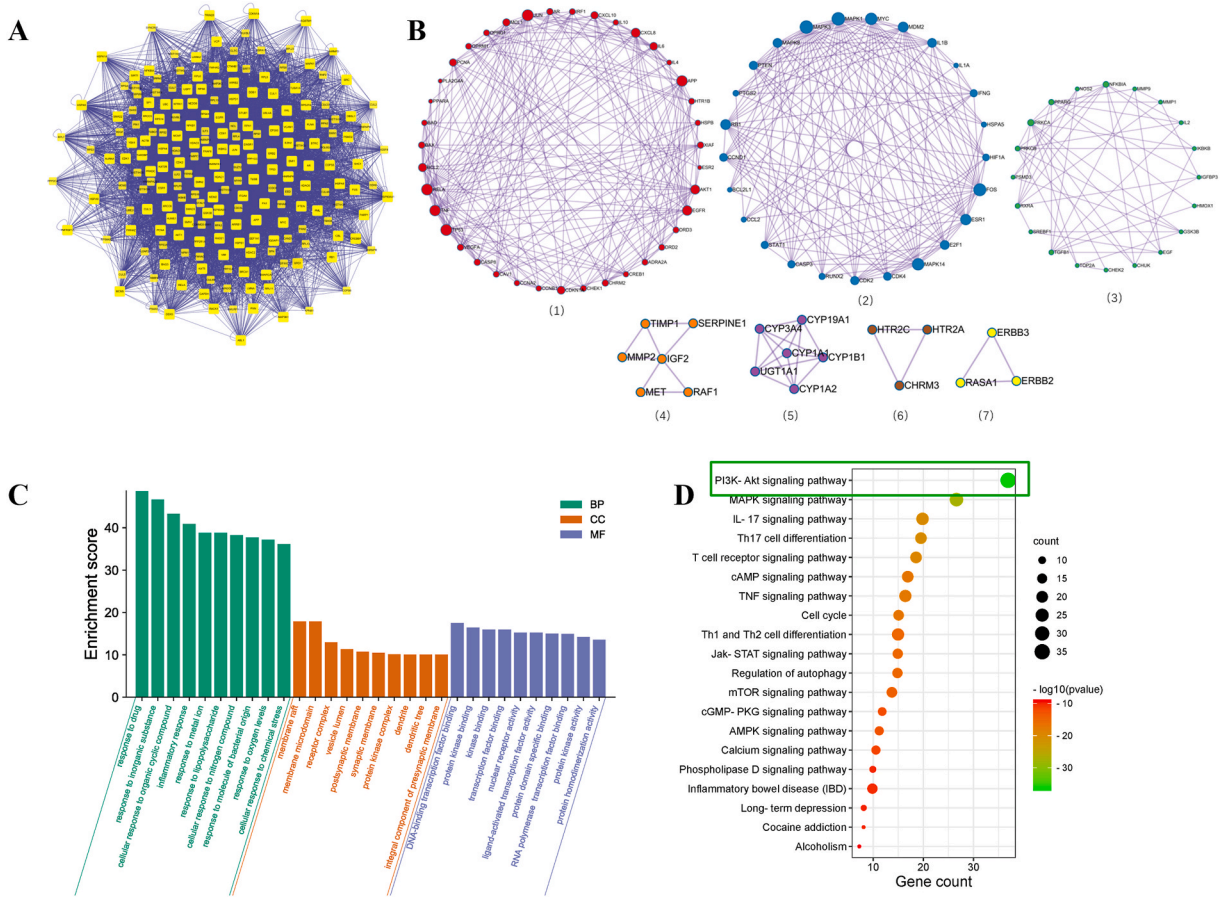

Fig. 2. Acquisition of key targets for BSTM treatment of STC. A, Core target interaction network of BSTM; B, Protein interaction diagram of the key target for BSTM treatment of STC; C, GO analyze of the key target for BSTM treatment of STC; D, KEGG analyze of the key target for BSTM treatment of STC.

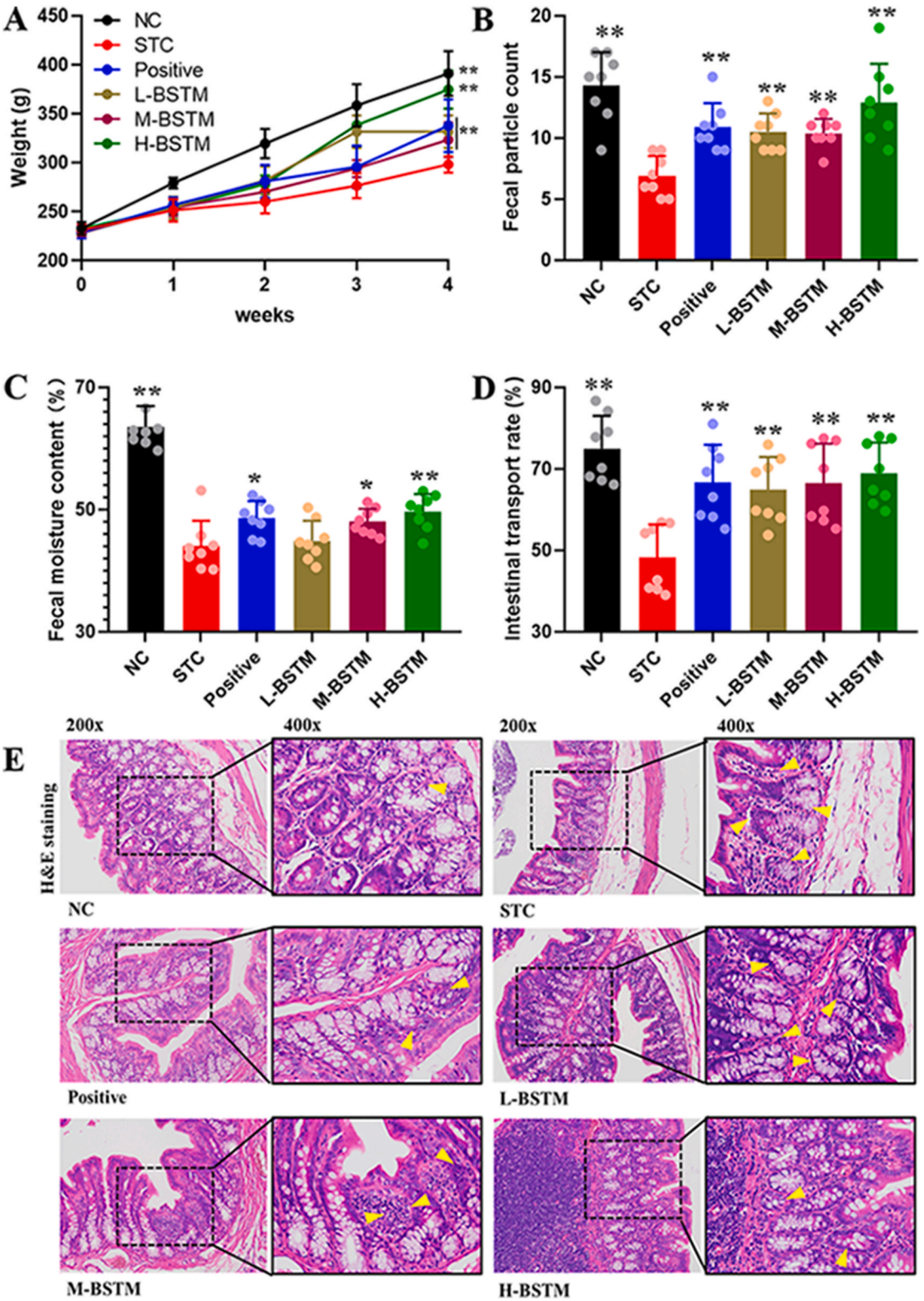

Fig. 3. BSTM improves constipation symptoms in STC rats. A, BSTM improves body weight loss in STC rats; B, BSTM increased the 24h fecal quantity of STC rats; C, BSTM increased fecal water content of STC rats; D, BSTM improves intestinal propulsion in STC rats; E, BSTM improved the pathological changes of colon in STC rats. $P < 0.05$, *, $P < 0.01$, **, vs STC group.

3.8. Effect of BSTM on the colonic morphology of STC rats

Histopathological analysis of colonic tissue from the NC group revealed that the colonic tissue had complete layers, namely the mucosa, submucosa, muscle layer and outer membrane; the mucosa was covered with a single layer of columnar epithelial cells, and

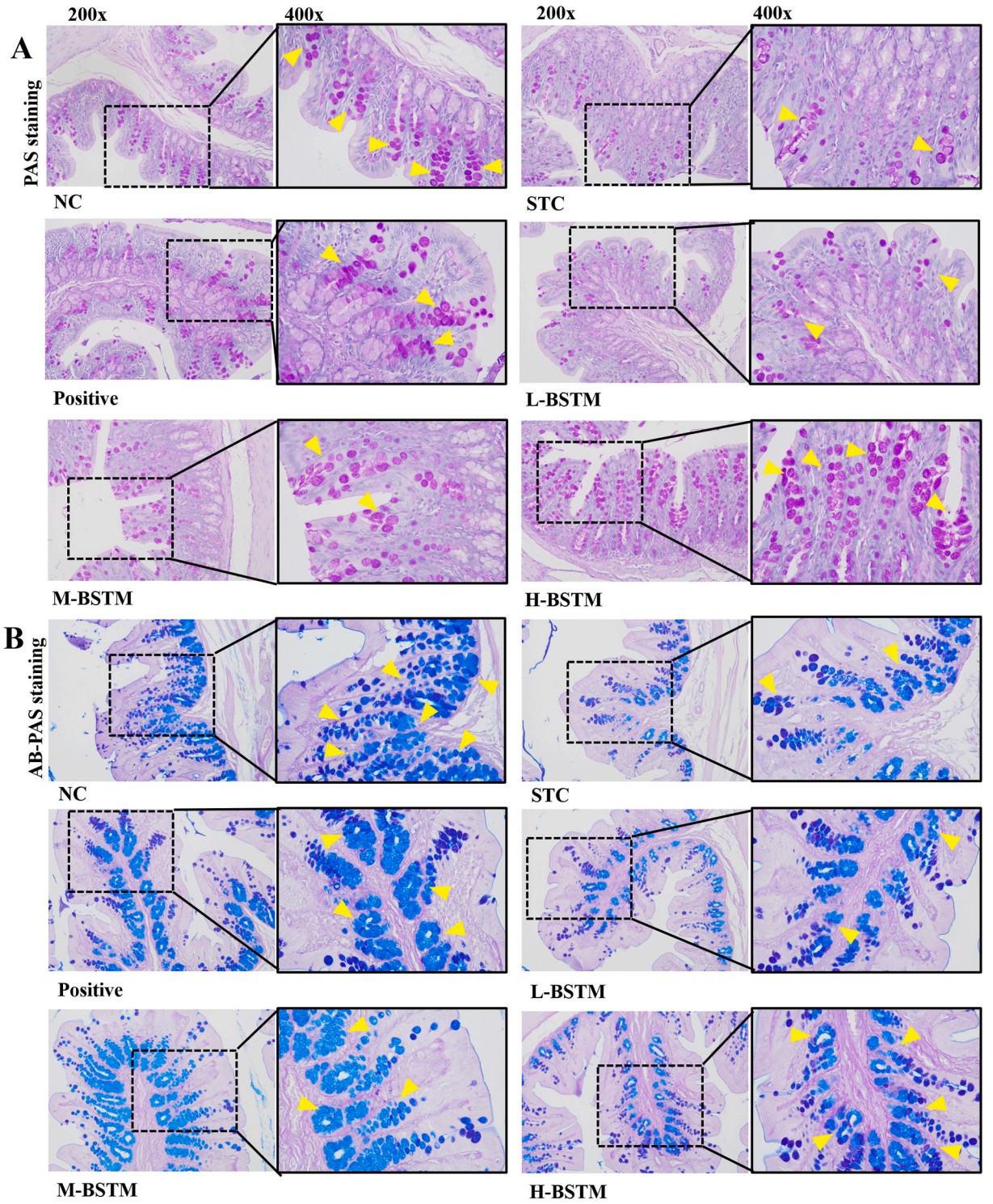

Fig. 4. BSTM increased the number of goblet cells in the colon of STC rats. A, PAS staining results; B, AB-PAS staining results. $P < 0.05$, *, $P < 0.01$, **, vs STC group.

many intestinal glands could be observed in the lamina. In the model group, mucosal necrosis, epithelial cell loss in the necrotic area, intestinal gland necrosis in the lamina propria, tubular structure loss, necrotic cell fragmentation and a few lymphocytes or neutrophils were observed. After treatment with BSTM and the positive control drugs, the degree of colon tissue injury improved significantly. The structure of the colon was relatively complete, the epithelial cells were more neatly arranged, and the lamina propria exhibited only slight intestinal gland necrosis and mild inflammatory cell infiltration (Fig. 3E). In addition, the number of colonic goblet cells was determined using PAS (Fig. 4A) and AB staining (Fig. 4B). The analysis showed that, compared with that in the NC group, the number of tissue goblet cells in the model group was significantly lower. However, these effects were significantly reversed after treatment with different doses of BSTM (Fig. 4).

3.9. BSTM reduces ICC apoptosis in rat colon tissue

As shown in Fig. 5, TUNEL-positive cells exhibited green fluorescence, c-Kit was used to label ICCs, and positive c-Kit expression was indicated by red fluorescence. Apoptosis of ICC apoptosis was not detected in the colonic tissues of the NC group. Compared with that in the NC group, ICC apoptosis was increased in the model group, but ICC apoptosis was decreased in all the dose groups treated with BSTM and in the positive control group, and ICC apoptosis was most significantly reduced in the high-dose BSTM group (Fig. 5A). Similarly, WB analysis revealed that the expression of c-kit, which is a hallmark protein of ICC, was significantly decreased in the colon of the model group of rats, while the positive control and BSTM treatment significantly increased the expression of c-kit in the colon (Fig. 5B & Fig. S1). Furthermore, apoptosis-related proteins in the colon of the rats were detected. As shown in Fig. 5C–D and Fig. S1, the expression of the proapoptotic proteins c-Caspase 3 and Bax in the colon of rats in the model group was significantly increased, and intervention with the positive control drugs and BSTM significantly alleviated this phenomenon. Moreover, the expression level of the antiapoptotic protein Bcl-2 in the colon was also significantly lower in the model group. Fortunately, combination therapy with drugs and BSTM could significantly increase the expression of Bcl-2.

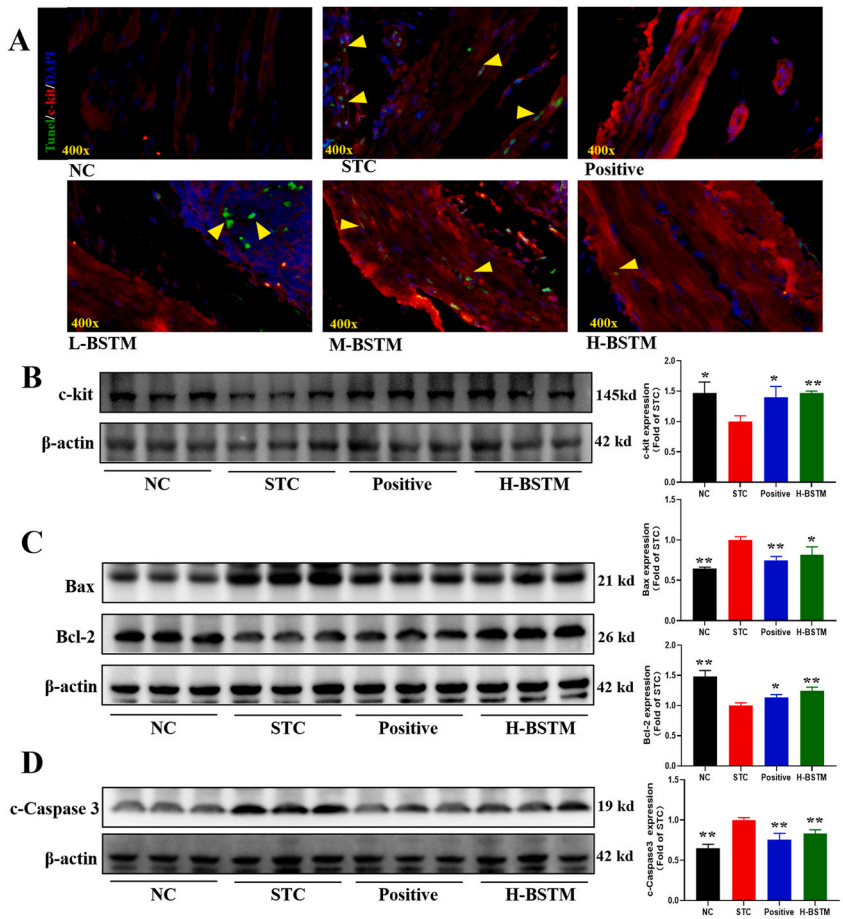

Fig. 5. BSTM inhibits the apoptosis of ICC cells in colon tissue of STC rats. A, Tunel staining and c-kit fluorescence staining of rat colon tissue; B, BSTM increased the expression of c-kit protein in the colon of STC rats; C, BSTM increased the expression of Bcl-2 protein and decreased the expression of BAX protein in the colon of STC rats; D, BSTM decreased the expression of c-Caspase 3 protein in the colon of STC rats. $P < 0.05$, *, $P < 0.01$, **, vs STC group.

3.10. BSTM reduces cell apoptosis by activating the PI3K/AKT pathway in ICC in rat colon tissue

Network pharmacology analysis predicted that the mechanism by which BSTM improved STC was related to the PI3K/AKT pathway. Therefore, we also detected the expression of PI3K and AKT pathway proteins in rat colon tissues. As shown in Fig. 6 compared with those in the NC group, the phosphorylation levels of PI3K and AKT in the colon tissue of rats in the model group were significantly lower, indicating that loperamide treatment could inhibit the activation of the PI3K/AKT pathway in the colon. However, BSTM intervention significantly increased the phosphorylation of PI3K and AKT in the colon of rats, which was consistent with the predicted network pharmacology results (Fig. 6 & Fig. S2).

3.11. BSTM component analysis

The chemical components of BSTM were analyzed by HPLC–MS. Eight components of BSTM were identified by comparison of their ion fragments, namely, arginine, decaffeoylacteoside, darendoside B, Jionoside A1/A2, acetoside, rehmapicrogenin, angoroside C, and harpagoside, as shown in Fig. 7A and B and Table S2 [18–21].

4. Discussion

STC is a common clinical disease, and its complex pathogenesis limits its progress in prevention, diagnosis and treatment. Traditional Chinese medicine has shown unique advantages in the prevention and treatment of STC. Studies have shown that *Atractylodes macrocephala Koidz.* and Magnolia officinalis Rehd. et Wils. contain volatile oils, lactones, flavonoids and other active ingredients, and their combination can promote gastrointestinal motility to play a laxative role by restoring the number and distribution of Cajal interstitial cells [22–24]. The BSTM is composed of Zhizhu Pill plus *Magnolia officinalis Rehd. et Wils.* (HP), *Rehmannia.* (SDH) and has definite clinical efficacy in the treatment of constipation [10]. To further clarify the specific mechanism by which BSTM alleviates STC, this study used network pharmacology to analyze the possible molecular mechanism by which BSTM treats STC and verified this mechanism through animal experiments. According to our network pharmacology analysis, the main components of BSTM involved in the treatment of STC were volatile oils, flavonoids, lactones and polysaccharides. Many studies have shown that volatile oils, flavonoids and other substances can improve the gastric emptying and intestinal propulsion of rats with functional dyspepsia, increase the release of endogenous motilin (MTL), promote gastric emptying in rats, and enhance intestinal propulsion [25–28]. The mechanism of action of Atractylodes macrocephala Koidz has been reported. The ability of BZ and Citrus aurantium L. (ZS) to treat STC may be related to restoring the number and distribution of ICCs, regulating the content of neurotransmitters in the ENS, promoting gastrointestinal motility, and regulating the expression of AQPs [29]. KEGG pathway enrichment analysis suggested that the molecular mechanism of BSTM therapy for STC may be closely related to the PI3K-Akt signaling pathway. The PI3K-Akt pathway is involved in

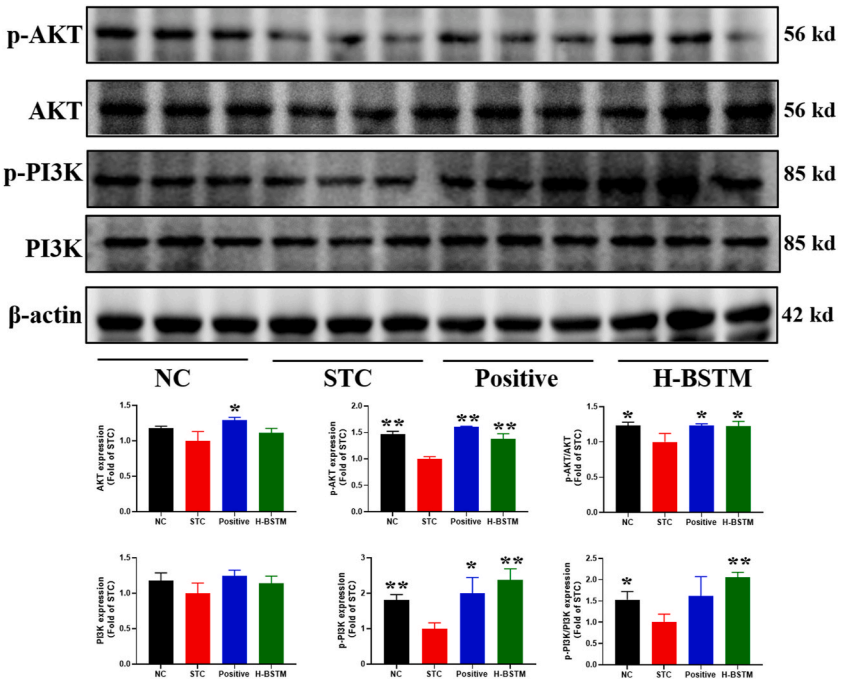

Fig. 6. BSTM activates PI3K/AKT pathway in colon tissue of STC rats and promotes AKT and PI3K phosphorylation. $P < 0.05$, *, $P < 0.01$, **, vs STC group.

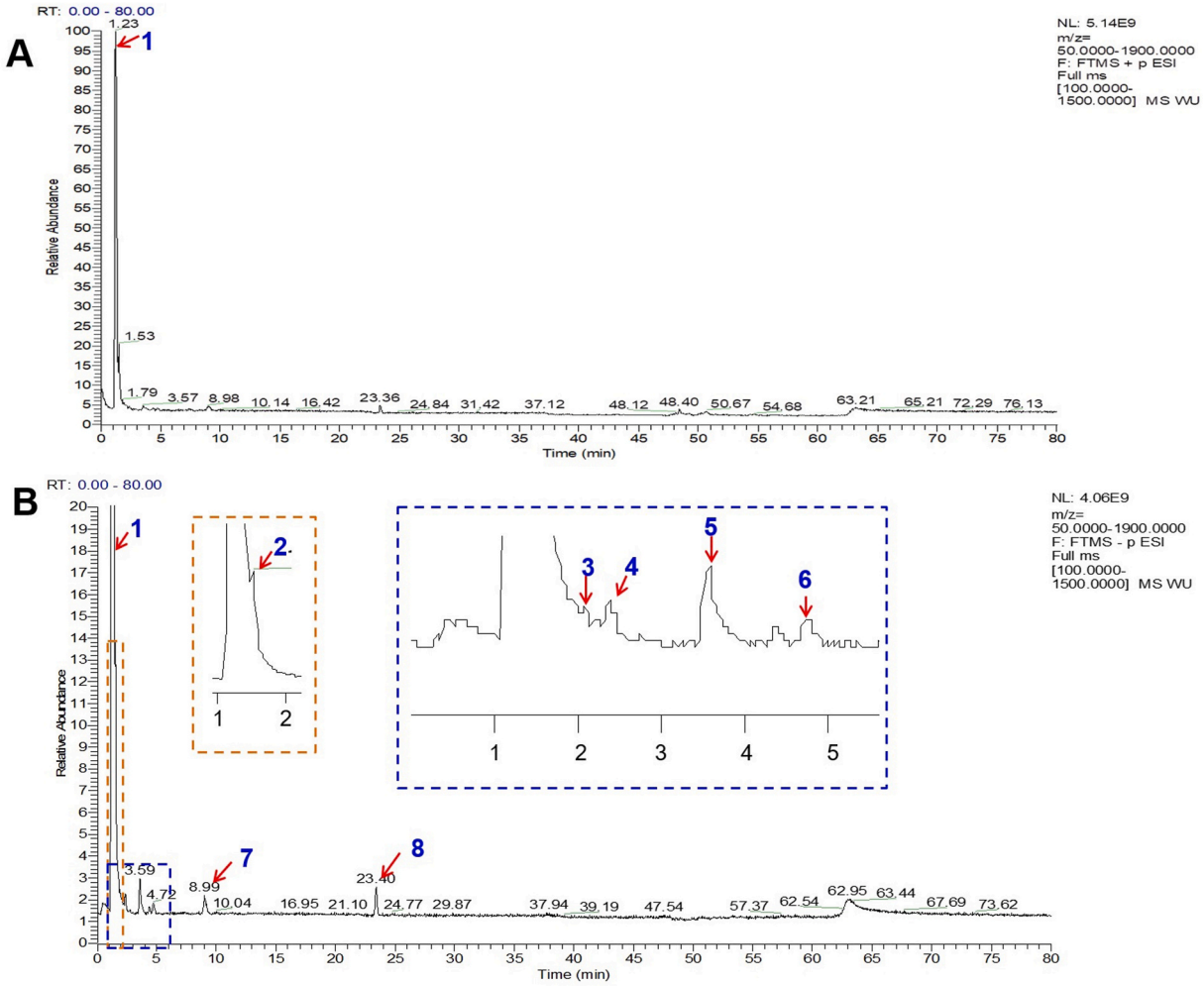

Fig. 7. Results of HPLC-MS identification of BSTM. A, HPLC-MS $^{+}$ESI spectrum of BSTM; B, HPLC-MS $^{-}$ESI spectrum of BSTM.

the regulation of cell proliferation and plays an extremely important role in promoting cell growth and inhibiting apoptosis, angiogenesis, and autophagy [30]. Moreover, the AKT signaling pathway can induce the secretion of the cytokines IL-6, IL-12 and TNF-α [31,32]. When the intestinal barrier function of rats is impaired, the serum inflammatory cytokines IL-6 and TNF-α are significantly increased.

ICCs generate slow waves, induce excitation and regulate neurotransmitters [33,34]. A decrease in or dysfunction of the ICC leads to a decrease in colon slow wave activity, blocks information transmission between the ENS and smooth muscle cells, delays electrical excitation transmission between pacemaker cells and smooth muscle cells, and leads to a decrease in the contractility of smooth muscle cells [35,36]. This results in colonic dyskinesia and delayed delivery of intestinal contents [37,38]. Therefore, ICCs are closely related to constipation. In animal experiments, the colonic Cajal mesenchymal cells of STC rats were shown to not function normally, and the apoptosis of colonic ICCs from rats in the model group was detected via TUNEL staining and immunofluorescence. Moreover, WB experiments showed that the expression of c-Kit (c-Kit is expressed mainly by ICCs in the intestine) was significantly decreased in the model group, the expression of the proapoptotic proteins Caspase 3 and Bax in the colon was significantly decreased, and the expression of the antiapoptotic protein Bcl2 was significantly increased, indicating that BSTM could upregulate the expression of c-Kit in colon tissue. Inhibition of ICC apoptosis. Apoptosis of ICCs in colon tissue is an important factor affecting the occurrence and development of STC [15]. Apoptosis is a programmed cell death process regulated by a variety of signaling molecules that trigger cascade reactions and lead to cell death [39]. The c-Caspase-3, Bax and Bcl-2 proteins play important roles in apoptosis [40]. In the present study, an STC rat model was established with loperamide, and after intervention with BSTM, the expression of c-caspase-3 and Bax was downregulated, that of Bcl-2 was upregulated, and that of key proteins in the PI3K/AKT pathway was significantly increased, which was highly consistent with the results predicted by network pharmacology. These results indicate that the laxative effect of BSTM is closely related to its antiapoptotic mechanism.

5. Conclusions

In summary, for the first time, this study used integrated network pharmacology and partial experimental verification methods to initially explore the possible mechanism of BSTM treatment, which may be related to the inhibition of the PI3K-Akt signaling pathway to improve Cajal cell apoptosis, providing an important direction and reference for further elucidating its pharmacological mechanism in detail. In this study, the PI3K/AKT pathway, which is the most enriched signaling pathway, was selected according to the prediction results of previous network pharmacology studies. The PI3K/AKT pathway is one of the most important signaling pathways involved in cell survival. Harpagoside, rehmapicrogenin, angoroside C and other components of BSTM inhibited apoptosis by inhibiting the production of intracellular ROS and activating the PI3K/AKT pathway [41–43]. Arginine modulates intestinal cell restitution by transforming growth factor-β1 [44,45]. Acetoside regulates NF-κB signaling in cells, suggesting its anti-inflammatory activity [46]. These studies suggest that BSTM may improve STC more than just regulate the PI3K/AKT pathway. In fact, our prediction results also suggest that the effect of BSTM on STC is related to the MAPK pathway, the IL-17 pathway, etc. STC is closely related to apoptosis, injury and inflammation in intestinal cells, and MAPK, IL-17 and other pathways play important roles in the above pathological activities of cells. In future research, we will further explore whether the anti-STC effect of BSTM is related to these pathways.

Consent to publish

All authors consent to publish.

Data availability statement

Data will be made available on request.

CRediT authorship contribution statement

Rong Wu: Writing – original draft, Software, Project administration, Methodology, Formal analysis, Data curation, Conceptualization. **Zhibin Zhang:** Writing – original draft, Supervision, Software, Methodology, Investigation. **Qingxia Xu:** Validation, Supervision, Project administration. **Fang Liu:** Software, Investigation, Formal analysis. **Yu Zhan:** Visualization, Supervision, Software. **Qiuxiao Wang:** Visualization. **Lijuan Du:** Writing – review & editing, Supervision, Funding acquisition. **Xuegui Tang:** Writing – review & editing, Supervision, Project administration, Funding acquisition.

Declaration of competing interest

The authors declare that they have no known competing financial interests or personal relationships that could have appeared to influence the work reported in this paper.

Funding Acknowledgments

This research was funded by the National Natural ScienceFoundation project (No. 82074429).

List of abbreviations

BSTM	Bian-Se-Tong mixture
STC	slow-transit constipation
TCM	Traditional Chinese medicine
LOP	Loperamide
OB	bioavailability
DL	drug-likeness
DC	connectivity centrality
BC	mediocrity centrality
CC	compactness centrality
GO	Gene Ontogy
KEGG	Kyoto Encyclopedia of Genes and Genomes
PAS	Periodate Schiff
IF	immunofluorescence staining
HE	hematoxylin-eosin

Appendix A. Supplementary data

Supplementary data to this article can be found online at https://doi.org/10.1016/j.heliyon.2024.e28022.

References

[1] J.E. Shin, K.S. Park, K. Nam, Chronic functional constipation, Korean J. Gastroenterol. 73 (2019) 92–98.
[2] M.J. Van Mill, I.J.N. Koppen, M.A. Benninga, Controversies in the management of functional constipation in children, Curr. Gastroenterol. 21 (1) (2019) 23.
[3] B. Barberio, C. Judge, E.V. Savarino, et al., Global prevalence of functional constipation according to the rome criteria a systematic review and Meta-analysis, Lancet. Gastroenterol. Hepatol. 6 (8) (2021) 638–648.
[4] V.J. Horváth, H. Vittal, A. Lörincz, et al., Reduced stem cell factor links smooth myopathy and loss of interstitial cells of Cajal in murine diabetic gastroparesis, Gastroenterology 130 (3) (2006) 759–770.
[5] J. Serra, D. Pohl, F. Azpiroz, et al., European society of neurogastroenterology and motility guidelines on functional constipation in adults, Neuro Gastroenterol. Motil. 32 (2) (2020) e13762.
[6] H. Zheng, Y.J. Liu, Z.C. Chen, et al., miR-222 Regulates cell growth, apoptosis, and autophagy of interstitial cells of Cajal isolated from slow transit constipation rats by targeting c-Kit, Indian J. Gastroenterol. 40 (2) (2021) 198–208.
[7] F. Zhu, S. Xu, Y. Zhang, et al., Total glucosides of paeony promote intestinal motility in slow transit constipation rats through amelioration of interstitial cells of Cajal, PLoS One 11 (8) (2016) e0160398.
[8] Q. He, C. Han, L. Huang, et al., Astragaloside IV alleviates mouse slow transit constipation by modulating gut microbiota profile and promoting butyric acid generation, J. Cell Mol. Med. 24 (16) (2020) 9349–9361.
[9] W.C. Gu, C. Chen, Y.M. Son, et al., Application of network pharmacology in the study of TCM compounds, Phytomedicine 40 (3) (2021) 662–667.
[10] X.G. Tang, J.Y. Tang, Z.J. Wu, Clinical observation of Biansaitong mixture in treating senile constipation, Chin. Patent. Med. 12 (10) (2006) 1767–1769.
[11] X.G. Tang, J. Wu, F. Liu, Experimental study on the regulation of GAS, MTL and SP in serum of rats with chronic constipation by Biansaitong Mixture, J. Chin. Med. 29 (2) (2011) 1549–1551.
[12] Q. Zhang, R. Li, W. Peng, et al., Identification of the active constituents and significant pathways of Guizhi-Shaoyao-Zhimu decoction for the treatment of diabetes mellitus based on molecular docking and network pharmacology, Comb. Chem. High Throughput Screen. 22 (9) (2019) 584–598.
[13] J. Ru, P. Li, J. Wang, et al., TCMSP a database of systems pharmacology for drug discovery from herbal medicines, J. Cheminf. 6 (6) (2014) 13.
[14] L. Ma, G.X. Tian, H. Geng, et al., A brief introduction to TCMSP and its analytical application, Chinn. J. evidence-based. Cardiovascular. Med. 12 (2) (2020) 1413–1416.
[15] M.M. Zhang, D. Wang, F. Lu, et al., Identification of the active substances and mechanisms of ginger for the treatment of colon cancer based on network pharmacology and molecular docking, BioData Min. 14 (1) (2021) 1.
[16] M.Y. Li, X.L. Zhu, B.X. Zhao, et al., Adrenomedullin alleviates the pyroptosis of Leydig cells by promoting autophagy via the ROS-AMPK-mTOR axis, Cell Death Dis. 10 (7) (2019) 489.
[17] W. Peng, C.X. He, R.L. Li, et al., Zanthoxylum bungeanum amides ameliorates nonalcoholic fatty liver via regulating gut microbiota and activating AMPK/Nrf 2 signaling, J. Ethnopharmacol. 318 (Pt A) (2024) 116848.
[18] F.Y. Yang, R.L. Xu, W. Niu, et al., Chemical composition analysis of classic famous decoction standard solution UPLC-Q-TOF-MS, Chin. J. Tra. Chin. Med. 47 (5) (2022) 2134–2147.
[19] M.X. Tan, J.L. Chen, L.S. Zou, et al., Comparative analysis of multivariate components of radix liopogon and radix liopogon, Chin. J. Tra. Chin. Med. 43 (2) (2018) 4084–4092.
[20] S. Chang, M. Wang, Y. Tian, et al., Systematic analysis and identification of the absorption and metabolic components of Zengye decoction in type 2 diabetic rats by HPLC-ESI-Q-TOF-MS/MS, Chin. Med. 15 (2020) 50.
[21] Y. Wu, Z.H. Qiu, W.J. Bai, et al., UPLC-Q-TOF-MS method for rapid analysis of chemical composition of Xuanmaiganjie particle, J. Chin. Experimental. Formulae. 23 (1) (2017) 70–76.
[22] M. Yang, Q. Zhang, R. Taha, et al., Polysaccharide from Atractylodes macrocephala Koidz. ameliorates DSS-induced colitis in mice by regulating the Th17/Treg cell balance, Front. Immunol. 13 (2022) 1021695.
[23] H. Cheng, D. Zhang, J. Wu, et al., Atractylodes macrocephala Koidz. volatile oil relieves acute ulcerative colitis via regulating gut microbiota and gut microbiota metabolism, Front. Immunol. 14 (2023) 1127785.
[24] C. Liu, S. Wang, Z. Xiang, et al., The chemistry and efficacy benefits of polysaccharides from Atractylodes macrocephala Koidz, Front. Pharmacol. 13 (2022) 952061.
[25] Y.L. Zhang, T. Lu, Y. Dong, et al., Auricular vagal nerve stimulation enhances gastrointestinal motility and improves interstitial cells of Cajal in rats treated with loperamide, Neuro Gastroenterol. Motil. 33 (10) (2021) e14163.
[26] L.P.H. Bastos, B.S. Costa, R.P. Siqueira, et al., Complex coacervates of β-lactoglobulin/sodium alginate for the microencapsulation of black pepper (Piper nigrum L.) essential oil Simulated gastrointestinal conditions and modeling release kinetics, Int. J. Biol. Macromol. 160 (2020) 861–870.
[27] L. Wu, L. Gao, X. Jin, et al., Ethanol extract of Mao Jian green tea attenuates gastrointestinal symptoms in a rat model of irritable bowel syndrome with constipation via the 5-hydroxytryptamine signaling pathway, Foods 12 (5) (2023) 1101.
[28] L. Wu, X. Jin, C. Zheng, et al., Bidirectional effects of Mao Jian green tea and its flavonoid glycosides on gastrointestinal motility, Foods 12 (4) (2023) 854.
[29] Y.X. Meng, X.X. Li, X. Wang, et al., Network pharmacological prediction and molecular docking analysis of the combination of Atractylodes macrocephala Koidz. and Paeonia lactiflora Pall. in the treatment of functional constipation and its verification, Animal. Model. Exp. Med. 5 (2) (2022) 120–132.
[30] Q. Zhang, D. Qian, D.D. Tang, et al., Glabridin from Glycyrrhiza glabra possesses therapeutic role against keloid via attenuating PI3K/Akt and TGF-β1/SMADs signalling pathways, J. Agric. Food Chem. 70 (35) (2022) 10782–10793.
[31] J. Yang, M. Cheng, B. Gu, et al., CircRNA_09505 aggravates inflammation and joint damage in collagen-induced arthritis mice via miR-6089/AKT1/NF-κB axis, Cell Death Dis. 11 (10) (2020) 833.
[32] Z. Chen, H. Wu, W. Fan, et al., Naringenin suppresses BEAS-2B-derived extracellular vesicular cargoes disorder caused by cigarette smoke extract thereby inhibiting M1 macrophage polarization, Front. Immunol. 13 (2022) 930476.
[33] Q.C. Xu, Y.C. Tien, Y.H. Shi, et al., METTL3 promotes intrahepatic cholangiocarcinoma progression by regulating IFIT2 expression in an m6A-YTHDF2-dependent manner, Oncogene 41 (11) (2022) 1622–1633.
[34] W. Cai, R. Makwana, M. Straface, et al., Evidence for tetrodotoxin-resistant spontaneous myogenic contractions of mouse isolated stomach that are dependent on acetylcholine, Br. J. Pharmacol. 179 (6) (2022) 1187–1200.
[35] B.T. Drumm, C.A. Cobine, S.A. Baker, Insights on gastrointestinal motility through the use of optogenetic sensors and actuators, J. Physiol. 600 (13) (2022) 3031–3052.
[36] G.Y. Zhu, D.D. Jia, Y. Yang, et al., The effect of Shaoyao Gancao decoction on sphincter of oddi dysfunction in hypercholesterolemic rabbits via protecting the enteric nervous system-interstitial cells of Cajal-smooth muscle cells network, J. Inflamm. Res. 14 (2021) 4615–4628.
[37] Y.B. Wang, J. Ling, W.Z. Zhang, et al., Effect of bisacodyl on rats with slow transit constipation, Braz. J. Med. Biol. Res. 51 (7) (2018) e7372.
[38] J.Y. Joung, S.H. Choi, C.G. Son, Interstitial cells of Cajal Potential targets for functional dyspepsia treatment using medicinal natural products, Evid. Based. Complement. Alternat. Med. 2021 (2021) 9952691.
[39] Q. Zhang, J. Liu, M.M. Zhang, et al., Apoptosis induction of fibroblast-like synoviocytes is an important molecular mechanism for herbal medicine and its active components to treat rheumatoid arthritis, Biomolecules 9 (12) (2019) 795.
[40] S.H.M. Pang, J. D'Rozario, S. Mendonca, et al., Mesenchymal stromal cell apoptosis is required for their therapeutic function, Nat. Commun. 12 (1) (2021) 6495.
[41] Y.W. Lu, R.J. Hao, Y.Y. Wei, et al., The protective effect of harpagoside on angiotensin II (Ang II)-induced blood-brain barrier leakage in vitro, Phytother Res. 35 (11) (2021) 6241–6254.
[42] M. Wang, Y. Ke, Y. Li, et al., The nephroprotective effects and mechanisms of rehmapicrogenin include ROS inhibition via an oestrogen-like pathway both in vivo and in vitro, Biomed. Pharmacother. 138 (2021) 111305.

[43] M. Liao, Q. Xie, Y. Zhao, et al. Main active components of Si-Miao-Yong-An decoction (SMYAD) attenuate autophagy and apoptosis via the PDE5A-AKT and TLR4-NOX4 pathways in isoproterenol (ISO)-induced heart failure models. Pharmacol. Res. 176 106077.
[44] M. Luo, Y. Zheng, S. Tang, et al., Radical oxygen species: an important breakthrough point for botanical drugs to regulate oxidative stress and treat the disorder of glycolipid metabolism, Front. Pharmacol. 14 (2023) 1166178.
[45] T. Matsui, H. Ichikawa, T. Fujita, et al. Histidine and arginine modulate intestinal cell restitution via transforming growth factor-β1. Eur. J. Pharmacol. 850 35-42.
[46] X. Shen, T. Eichhorn, H.J. Greten, et al., Effects of scrophularia ningpoensis hemsl. On inhibition of proliferation, apoptosis induction and NF-κB signaling of immortalized and cancer cell lines, Pharmaceuticals 5 (2) (2012) 189–208.